Water Research 196 (2021) 117003

Contents lists available at ScienceDirect

Water Research

journal homepage: www.elsevier.com/locate/watres

# Biotransformation of lincomycin and fluoroquinolone antibiotics by the ammonia oxidizers AOA, AOB and comammox: A comparison of removal, pathways, and mechanisms

Li-Jun Zhou[a], Ping Han[b,c,d,*], Mengyue Zhao[b], Yaochun Yu[e,f], Dongyao Sun[b], Lijun Hou[c], Min Liu[b,d], Qiang Zhao[b], Xiufeng Tang[b], Uli Klümper[g], Ji-Dong Gu[h], Yujie Men[e,f], Qinglong L. Wu[a,i]

[a] State Key Laboratory of Lake Science and Environment, Nanjing Institute of Geography and Limnology, Chinese Academy of Sciences, Nanjing, 210008, China
[b] School of Geographic Sciences, East China Normal University, 500 Dongchuan Road, Shanghai 200241, China
[c] State Key Laboratory of Estuarine and Coastal Research, East China Normal University, 500 Dongchuan Road, Shanghai 200241, China
[d] Institute of Eco-Chongming, East China Normal University, 3663 North Zhongshan Road, Shanghai 200062, China
[e] Department of Civil and Environmental Engineering, University of Illinois at Urbana-Champaign, Urbana, Illinois 61801, United States
[f] Department of Chemical and Environmental Engineering, University of California, Riverside, California 92521, United States
[g] Institute for Hydrobiology, Technische Universität Dresden, Dresden 01217, Germany
[h] Environmental Engineering, Guangdong Technion - Israel Institute of Technology, 241 Daxue Road, Shantou, Guangdong 515063, China
[i] Sino-Danish Center for Science and Education, University of Chinese Academy of Sciences, Beijing, China

ARTICLE INFO

*Article history:*
Received 18 December 2020
Revised 1 March 2021
Accepted 2 March 2021
Available online 3 March 2021

*Keywords:*
Ammonia oxidizers
biotransformation
comammox
cometabolism
lincomycin
fluoroquinolones

ABSTRACT

In this study, we evaluated the biotransformation mechanisms of lincomycin (LIN) and three fluoroquinolone antibiotics (FQs), ciprofloxacin (CFX), norfloxacin (NFX), and ofloxacin (OFX), which regularly enter aquatic environments through human activities, by different ammonia-oxidizing microorganisms (AOM). The organisms included a pure culture of the complete ammonia oxidizer (comammox) *Nitrospira inopinata*, an ammonia oxidizing archaeon (AOA) *Nitrososphaera gargensis*, and an ammonia-oxidizing bacterium (AOB) *Nitrosomonas nitrosa* Nm90. The removal of these antibiotics by the pure microbial cultures and the protein-normalized biotransformation rate constants indicated that LIN was significantly co-metabolically biotransformed by AOA and comammox, but not by AOB. CFX and NFX were significantly co-metabolized by AOA and AOB, but not by comammox. None of the tested cultures transformed OFX effectively. Generally, AOA showed the best biotransformation capability for LIN and FQs, followed by comammox and AOB. The transformation products and their related biotransformation mechanisms were also elucidated. i) The AOA performed hydroxylation, S-oxidation, and demethylation of LIN, as well as nitrosation and cleavage of the piperazine moiety of CFX and NFX; ii) the AOB utilized nitrosation to biotransform CFX and NFX; and iii) the comammox carried out hydroxylation, demethylation, and demethylthioation of LIN. Hydroxylamine, an intermediate of ammonia oxidation, chemically reacted with LIN and the selected FQs, with removals exceeding 90%. Collectively, these findings provide important fundamental insights into the roles of different ammonia oxidizers and their intermediates on LIN and FQ biotransformation in nitrifying environments including wastewater treatment systems.



## 1. Introduction

Antibiotics are widely used to cure human and animal diseases, and are also used as feed additives to promote growth in animals (Kümmerer, 2009; Sarmah et al., 2006). Lincomycin (LIN) and fluoroquinolones (FQs) are the most widely used groups of antibiotics owing to their broad-spectrum activity against diverse bacteria. LIN and FQs have been frequently detected in wastewater treatment plants (WWTPs) (Rodriguez-Mozaz et al., 2015; Zhi et al., 2018; Zhou et al., 2013), rivers (Danner et al., 2019; Gao et al., 2012; Kümmerer, 2009; Mirzaei et al., 2019; Zhou et al., 2011), and lakes (Liu et al., 2018; Zhou et al., 2016; Zhou et al., 2019b), with concentrations ranging from ng/L to $\mu$g/L. Because of their low concentra-

* Corresponding author.
*E-mail address:* phan@geo.ecnu.edu.cn (P. Han).

https://doi.org/10.1016/j.watres.2021.117003
0043-1354/

tions in the environment, these pharmaceuticals are also referred to as micropollutants (MPs).

The presence of antibiotic MPs in the environment can have detrimental effects on ecosystems and human health owing to their recalcitrance. First, LIN and FQs may enhance the spread of antibiotic resistance genes (ARGs) and antibiotic resistance bacteria (ARBs) (Bengtsson-Palme and Larsson, 2016; Grenni et al., 2018; Klumper et al., 2019; Wang et al., 2020). Second, the continuous release of antibiotic MPs such as LIN and FQs into the environment can adversely affect the indigenous population of organisms. For example, LIN in the soil affected the denitrification process by inhibiting nitrite reduction (D'Alessio et al., 2019), and it markedly altered bacterial community composition (Wang et al., 2020). The presence of ciprofloxacin (CFX) at 0.1 $\mu$g/kg wet weight in sediment samples also affected the bacterial community structure (Naslund et al., 2008). CFX may further pose a series of adverse effects on diverse organisms, including *Drosophila melanogaster* (Liu et al., 2019), earthworm *Eisenia fetida* (Yang et al., 2020), cyanobacteria, and green algae (Gonzalez-Pleiter et al., 2013).

FQs are recalcitrant to biodegradation in water but are prone to adsorb into sediments in aquatic environments or sludge in WWTPs (Rusch et al., 2019). Owing to the negative effects of FQs and their transformation products (TPs) in the environment, the biodegradation of FQs by microorganisms, such as fungi and bacteria, has been widely studied (Brienza et al., 2020; Rusch et al., 2019). While several microorganisms can biodegrade FQs (Rusch et al., 2018; Rusch et al., 2019), few studies have focused on the biodegradation of FQs in nitrifying conditions (Rusch et al., 2019). Although LIN can be biodegraded in WWTPs (Zhou et al., 2013) and biological aerated filter system (Chen et al., 2017), few studies on LIN-biodegrading microorganisms or the degradation mechanisms are available. A LIN-degrading strain was isolated from the LIN mycelial residue, and the gene *lnuB* participated in LIN biodegradation based on the analysis of degradation products and pathways (Wang et al., 2018) Furthermore, co-metabolism technology was employed previously to degrade LIN in wastewater, resulting in the effective degradation of LIN functional groups (Li et al., 2016).

Ammonia oxidizers including AOA, AOB, and comammox are ubiquitous in various environments (Chao et al., 2016; Daims et al., 2015; Liu et al., 2020; Pjevac et al., 2017; Prosser and Nicol, 2012; Zhang et al., 2020; Zhao et al., 2020). In the nitrifying environments of WWTPs, AOB represent the majority of ammonia-oxidizing microorganisms (AOM) (Mussmann et al., 2011); AOA and comammox have also regularly been detected by cultivation or molecular tools (Chao et al., 2016; Daims et al., 2015; Pjevac et al., 2017; Sauder et al., 2017). Many MPs can be co-metabolically biotransformed by AOA, AOB, and comammox strains (Han et al., 2019; Yu et al., 2018; Zhou et al., 2019a), and the ammonia monooxygenases (AMOs) of AOM may potentially play an important role (Han et al., 2019; Yu et al., 2018; Zhou et al., 2019a). The three phylogenetically distant ammonia oxidizing groups have different transformation pathways of ammonia (i.e., comammox completely oxidizes ammonia to nitrate, whereas AOA and AOB only oxidize ammonia to nitrite) (Daims et al., 2015), enzymatic repertoires (Caranto and Lancaster, 2017; Daims et al., 2015; Vajrala et al., 2013), and ammonia affinities (Kits et al., 2017). These important differences may result in different metabolic activities transforming MPs (Han et al., 2019; Zhou et al., 2019a). FQs with piperazine rings and LIN with an amide moiety can be biodegraded by AOM according to previous studies (Helbling et al., 2010; Helbling et al., 2012). To date, there have been no studies on the biodegradation of FQs and LIN by these three different ammonia oxidizers.

The objective of the present study was to evaluate the biotransformation mechanisms of LIN and three FQs by three phylogenetically distant ammonia oxidizers. LIN and three typical FQs, CFX, norfloxacin (NFX), and ofloxacin (OFX), were selected for this study based on their frequent detection in WWTPs and aquatic environments. Three pure cultures of ammonia oxidizers including *N. gargensis* (an AOA strain), *N. nitrosa* Nm90 (an AOB strain), and *N. inopinata* (a comammox strain), were used to compare the biotransformation abilities of different ammonia oxidizers with different characteristics. Their TPs were identified using LC-HRMS/MS, which was used to analyze the proposed MP biotransformation pathways of the different ammonia oxidizers. The intermediate products hydroxylamine and nitric oxide of ammonia oxidation were also used to evaluate whether it could react abiotically with LIN and FQs.

## 2. Materials and methods

### 2.1. Antibiotic selection

The four antibiotics LIN, CFX, NFX, and OFX were chosen considering their high frequency of detection in WWTPs and natural environments (Danner et al., 2019; Kümmerer, 2009; Liu et al., 2018; Mirzaei et al., 2019; Zhou et al., 2016; Zhou et al., 2013; Zhou et al., 2011; Zhou et al., 2019b). Selected MPs were provided by Dr. Ehrenstorfer GmbH (Augsburg, Germany). Stock solutions of target compounds were prepared in methanol (MeOH) or ethanol (EtOH) (1 g/L) and stored at -20°C until use. The physicochemical properties of the target compounds are presented in Table S1 of Supporting Information (SI).

### 2.2. Cultivation of nitrifying strains

The details of the cultivation of the three nitrifying strains have been provided in our previous study (Zhou et al., 2019a). *Nitrososphaera gargensis*, an AOA, was isolated from the outflow of a hot spring (Hatzenpichler et al., 2008); *Nitrosomonas nitrosa* Nm90, an AOB strain, was isolated from WWTPs (Koops et al., 1991); *Nitrospira inopinata* (the only currently available comammox pure culture), was isolated from hot water (56°C, pH 7.5) raised from a 1,200 m deep oil exploration well (Daims et al., 2015). A modified basal medium adjusted to pH 8.0 using 4 M $CaCO_3$ was used in this study. The comammox strain, *N. inopinata*, and the AOA strain, *N. gargensis* were incubated at 42°C and 46°C in the dark, respectively. The AOB strain isolated, *Nitrosomomas nitrosa* Nm90, was incubated at 80 rpm and 37°C in the dark. A recently isolated AOB strain *Nitrosomomas nitrosa* 18-3D (Han et al., 2021) which has 100% 16S rRNA gene similarity with *N. nitrosa* Nm90 was also tested in individual-compound experiment. The two AOB strains showed similar MP biotransformation pattern thus we only described results for *N. nitrosa* Nm90 in the following sections. The basal medium was amended with $NH_4Cl$ (1 mM for comammox, 2 mM for AOA and AOB) once per week as growth substrate.

### 2.3. Biotransformation experiments

The target pollutant biotransformation capabilities of the three ammonia oxidizers (AOA, AOB, and comammox) were investigated using batch cultures. After incubation, the biomass was collected by centrifugation at 8,000 $\times$ *g* at 10°C for 30 min, then washed with fresh medium to remove nitrite/nitrate, and finally concentrated approximately 2 times. The initial concentrations of total protein in AOA, AOB and comammox treatments are 11.2 $\pm$ 1.48 mg/L, 7.8 $\pm$ 1.11 mg/L and 15.0 $\pm$ 1.98 mg/L, respectively. The stock solution of MPs was added into empty sterile bottles first to let organic solvents evaporate before adding culture. 25 mL prepared culture was transferred into 100 mL glass bottles. To avoid the toxicity of antibiotics on AOMs, the initial concentration of each compound in the experiments involving a mixture of antibiotic MPs

were adjusted to 20 μg/L. In the experiments involving a single antibiotic compound for TP analysis, to enhance the instrumental signals of TPs, the initial concentration of each compound was adjusted to 40 μg/L. The bottles were shaken at 80 rpm for ~ 20 min to re-dissolve the target compounds, and further incubated at the optimal growth temperatures of the corresponding ammonia oxidizers in the dark.

Liquid samples (~ 0.7 or 0.5 mL) were taken after biomass addition at 0 h, 16 h, 24 h, 48 h, 72 h, 96 h, 144 h, 7 d, 10 d, and 14 d for the mixed compound experiments, or every second day over a period of 14 days for those of individual compounds. Samples were centrifuged at 8000 × *g* for 10 min at 4°C. A 300 μL aliquot of the supernatant was transferred to a 2 mL- amber glass vial and kept at 4°C until LC-MS/MS analysis. The remaining supernatant was stored in 1.5 mL microcentrifuge tubes at 4°C, which was used for measuring ammonia and nitrite/nitrate concentrations. Cell pellets were stored at -20°C for measuring the total protein concentrations.

Abiotic control experiments carried out to investigate the hydrolysis and photodegradation of the parent compounds, and their sorption potential on $CaCO_3$ precipitates, were set up with the basal medium containing either 8 g/L or no $CaCO_3$. Heat-inactivated biomass controls were set up by inoculating the same amount of autoclaved (at 121°C and 103 kPa for 20 min for two cycles) culture. Successful inactivation of heat-inactivated biomass using the same protocol was already tested in our previous experiments based on no ammonia being used (Men et al., 2016). Ammonium (2 mM) and nitrite (6 mM) were amended to abiotic and heat-inactivated controls to investigate potential abiotic transformation of target compounds by nitrite. Biotic controls with active microbial biomass and $NH_4$-N only (without target MPs) were also set. All treatments were carried out in triplicate.

### 2.4. Role of hydroxylamine and nitric oxide in antibiotic transformation

Hydroxylamine ($NH_2OH$) and nitric oxide (NO) are ammonia oxidation intermediates by AOA, AOB and comammox. To evaluate their effects on transformation of antibiotics in the cultures of the ammonia oxidizers, transformation experiments with MPs after addition of $NH_2OH$ and NO were performed in sterile basal medium with 2 mM ammonia, according to the methodology of our previous paper (Yu et al., 2018). A mixture of all MPs was added to the sterile medium at an initial concentration of 20 μg/L for each compound. Then, 10 μM $NH_2OH$ was added to the medium every 12 h over a 168-h incubation period. NONOate (114.3 μM) was added to release NO (~200 μM during the 168-h incubation). Samples were collected at 0, 72, and 168 h for LC-HRMS analysis.

### 2.5. Analytical method of MPs by LC-HRMS/MS

For the experiments with mixed compounds, antibiotics were analyzed using a liquid chromatograph coupled to a high-resolution quadrupole orbitrap mass spectrometer (LC-HRMS) (Q Exactive, Thermo Fisher Scientific, Waltham, MA, USA). For LC analysis, 50 $\mu$L of the sample was injected and separated by a C18 Atlantis-T3 column (particle size 3 $\mu$m, 3.0 × 150 mm, Waters). The mobile phases were nanopure water (A) and acetonitrile (B) (both amended with 0.1% formic acid) eluted at a flow rate of 350 $\mu$L/min. The gradient elution started at 5% B for 1min, then changed to 100% B in 7 min and maintained for 12 min, and was finally changed to 5% B in 6 min and maintained for 6 min. The compound detection was completed in full scan mode on HRMS at a resolution of 70,000 at m/z 200 and a scan range of m/z 50 -750 in a ESI (+)/(-) switching mode.

For experiments with individual compounds, MPs were analyzed by Acquity I-class UPLC and Vion IMS QToF MS (Waters, MA, USA) using a C18 HSST3 column (particle size 1.7 $\mu$m, 2.1 × 100 mm, Waters). The mobile phases were nanopure water (A) and acetonitrile (B) (both amended with 0.1% formic acid). The injection volume was 5 μL, and the flow rate was 400 $\mu$L/min, with gradient elution (5% B, 0 - 2 min; linear gradient from 5 to 25% B, 2 - 5 min; 50% B, 5 - 7 min; 50 - 100% B, 7 - 10 min; 100% B, 10 - 12 min; and 95% B, 12 - 15 min); the initial conditions were restored for 3 min to equilibrate the column. The scan range was 50 - 1,000 m/z, and spectra were acquired in the positive-ion mode.

### 2.6. Transformation product identification

Suspect screening was carried out using TraceFinder 4.1 EFS software (Thermo Scientific, MA, USA). Suspect lists of potential TPs for target compounds were used, which considered a number of known redox, hydrolysis and conjugation reactions (Men et al., 2016). Suspected TPs with an intensity above a set threshold, > 70% match with the predicted isotopic patterns, and an increasing trend over the time course, were selected for further identification (Men et al., 2016).

Non-target screening was further performed to identify potential TPs. TP candidates were chosen following the criteria: (1) a reasonable peak shape and an intensity above noise; (2) presence in the antibiotic-added treatments and absence in non-antibiotic treatment; (3) a reasonable time-series pattern (i.e., increase, or increase and subsequent decrease during the experiment); and (4) a rational molecular formula originated from the exact mass of [M+H], [M+$NH_4$], [M+Na] or [M-$H_2O$+H] (with < 5 ppm tolerance) and isotopic pattern (isotope ratio difference < 10%). Because the reference standards for TP candidates were not commercially available, the peak area of TPs are only used to indicate the formation trend but not for quantification.

### 2.7. Calculation of kinetic parameters for MP biotransformation

Details of the calculation have been presented in our previous study (Zhou et al., 2019a). Considering that the growth substrate of ammonia oxidizers, ammonium, was unlimited, a First-order model was used in this study (Men et al., 2016). The protein-normalized biotransformation rate constants $k_{bio}$ were corrected for sorption and abiotic processes, and used to quantitatively compare the biotransformation activities among different treatments in this study. Moreover, only the time points that presented first-order kinetics according to the biotransformation curves were used for calculation (Figures S1-S3).

$$\frac{dS_c}{dt} = -f_{aq}(k_{bio}X + k_a) \times S_c \quad (1)$$

$$f_{aq} = \frac{S_c}{S_{ct}} \quad (2)$$

$$K_d = \frac{1 - f_{aq}}{f_{aq}X} \quad (3)$$

where $S_c$ is target compound's aqueous concentration, $f_{aq}$ is the dissolved fraction of target compound, $k_{bio}$ is the total protein concentration-normalized biotransformation rate constant, $X$ is the total protein concentration, $k_a$ is the abiotic transformation rate, $S_{ct}$ is target compound's total concentration, and $K_d$ is the sorption coefficient.

### 2.8. Ammonium, nitrite, and nitrate measurements

Ammonium ($NH_4^+$+$NH_3$) was analyzed using a colorimetric method (Kandeler and Gerber, 1988). Nitrite concentrations were

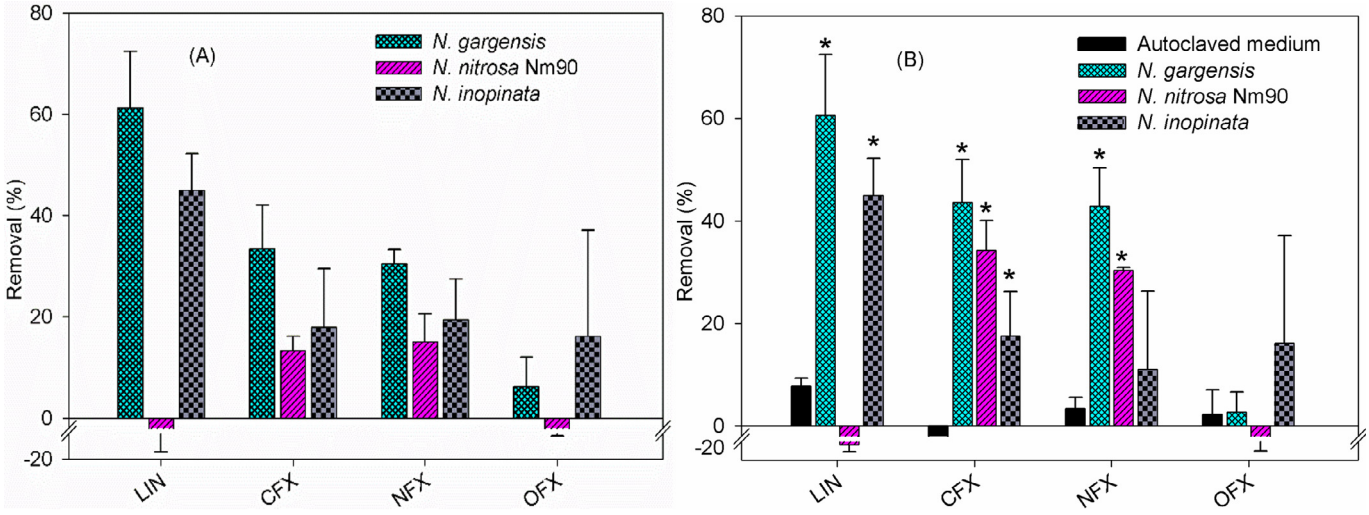


**Fig. 1.** Removal of the four MPs through biotransformation by *N. gargensis* (AOA), *N. nitrosa* Nm90 (AOB), and *N. inopinata* (comammox) ($n = 3$). Removal (%) was calculated by the following equation: removal (%) = $[(C_0\text{-}C_t)/C_0] \times 100\%$; $C_t$ and $C_0$ represent the concentrations of MPs at any sampling time T and the starting of the incubation, respectively. A) Removal by the AOA and AOB strains at 144 h, and by the comammox strain at 336 h. B) Removal by the AOA strain at 240 h, by the AOB strain at 504 h, and the comammox strain at 336 h. LIN, lincomycin; CFX, ciprofloxacin; NFX, norfloxacin; OFX, ofloxacin. For each compound in Fig. 1(B), asterisks on the columns indicate significant differences compared to the values in abiotic control with autoclaved medium (incubation by 504 h).

measured using the sulfanilamide N - (1-naphthyl) ethylenediamine dihydrochloride (NED) reagent method. Nitrate concentrations were investigated by being reduced into nitrite by vanadium chloride first and measured as $NO_x$ (Miranda et al., 2001).

### 2.9. Total protein measurement

Total protein concentration was analyzed using a Pierce BCA Protein Assay Kit (Thermo Scientific, Regensburg, Germany) according to the manufacturer's instructions.

## 3. Results and discussion

### 3.1. MP biotransformation by AOA, AOB and comammox pure cultures

First, the sorption of target compounds onto $CaCO_3$ precipitates and dead cells as well as their abiotic transformation in the basal medium was examined. No substantial sorption was detected; less than 7.75% ± 1.6% of the added MPs were abiotically degraded during an incubation time of 520 h (Fig. 1). Then, the antibiotic biotransformation abilities of the three ammonia oxidizers, AOA, AOB, and comammox, were evaluated (Fig. 1 and Figures S1-S3).

Compared to biotic controls with dead biomass, significant removals (end time point, two-tailed *t* test, $p < 0.05$) of LIN, CFX, and NFX by the AOA *N. gargensis* (incubation by 240 h) were observed, with removals ranging from 43% ± 8.4% to 61% ± 12%. For the AOB strain *N. nitrosa* Nm90 (incubation by 504 h), relatively low removals of CFX (34% ± 6%) and NFX (30% ± 0.6%) were observed. For comammox *N. inopinata* (incubation by 336 h), only LIN was removed (end time point, two-tailed *t* test, $p < 0.05$), with the removal of 45% ± 7.7% (Fig. 1B). When compared to abiotic controls with autoclaved fresh medium, LIN, CFX and NFX by the AOA *N. gargensis* (incubation by 240 h), CFX and NFX by the AOB *N. nitrosa* Nm90 (incubation by 504 h), LIN and CFX by the comammox *N. inopinata* (incubation by 336 h) were significantly removed (end time point, two-tailed *t* test, $p < 0.05$) (Fig. 1B). Protein-normalized biotransformation rates of LIN, CFX, and NFX by the three different groups of ammonia oxidizers were analyzed (Fig. 2). The protein-normalized biotransformation rate constants $k_{bio}$ of LIN, CFX, and NFX by the AOA strain *N. gargensis* (median value with 5%, 95% percentile in brackets) were 0.025 (0.016-0.047), 0.0072 (0.005-0.012), and 0.0068 (0.0048-0.011) L • (mg total protein)$^{-1}$(d)$^{-1}$, respectively (Fig. 2 and Table S2). The median $k_{bio}$ value of LIN by comammox *N. inopinata* was 0.0074 L • (mg total protein)$^{-1}$ • d$^{-1}$ with 5%-95% percentile 0.005-0.010 L • (mg total protein)$^{-1}$ • d$^{-1}$, hence lower than that of AOA. However, the biotransformation of CFX and NFX by the AOB strain *N. nitrosa* Nm90 cannot be fitted well with the model, which might be due to the lag phase (very low removals) at the beginning (Fig. S2). The removal and $k_{bio}$ values suggested that the AOA strain *N. gargensis* possessed the best biotransformation ability of LIN and FQs, followed by comammox and AOB used in this study. These results were consistent with those of the biotransformation of sulfonamides by the same pure AOA, AOB, and comammox cultures (Zhou et al., 2019a).

MP removals were also compared at the time when the same amount of ammonia (~5-6 mM) was oxidized by different ammonia oxidizers (Fig. 1A). After exhausting the same amount of ammonia, the AOA strain (144 h) showed the best removals of LIN, CFX, and NFX, followed by the comammox strain. However, no significant removal (≤ 20%) was observed for the target LIN and FQs by the AOB strain at 144 h. With the incubation time being extended to 504 h, the removals of CFX and NFX by the AOB strain gradually increased (Fig. 1B).

The different $k_{bio}$ values and biotransformation processes of LIN and FQs by the AOA, AOB, and comammox strains may have been cause by different physiological characteristics of these ammonia oxidizers, such as the substrate affinity and cell growth rate (Zhou et al., 2019a). For example, the ammonia affinities of ammonia oxidizers generally followed the order of: comammox > non-marine AOA > many AOB (He et al., 2012; Kits et al., 2017; Martens-Habbena et al., 2009). If MP biotransformation by ammonia oxidizers is carried out by the AOM, different substrate affinities for ammonia might result in different affinities for target MPs (Zhou et al., 2019a). The comammox cultures had lower nitrite/nitrate formation rates than AOA (Table S1), which indicated a lower growth rate and hence oxidation ability (i.e., oxidation of ammonia to nitrate). Generally, protein-normalized biotransformation rates and removals of LIN and FQs by ammonia oxidizers are lower than those of sulfonamides by ammonia oxidizers (Zhou et al., 2019a), which is probably related to the molecular structures of target MPs.

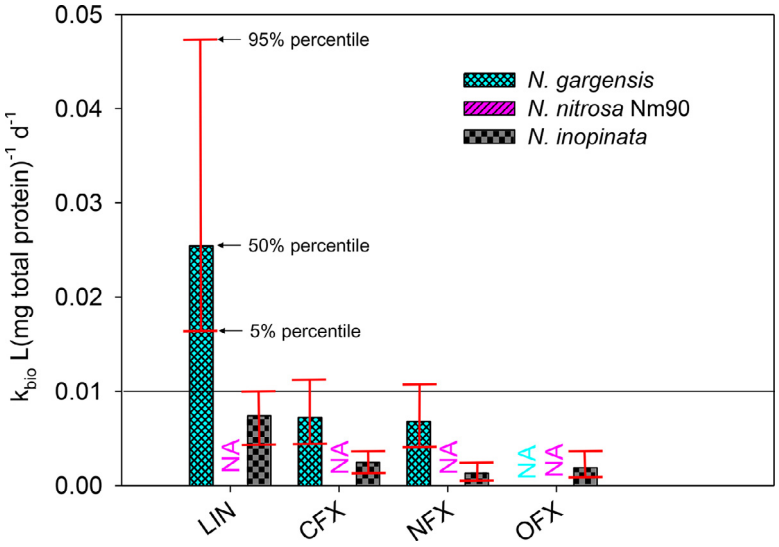


**Fig. 2.** First-order biotransformation rate constants ($k_{bio}$) of MPs by *N. gargensis*, *N. nitrosa* Nm90 and *N. inopinata*. LIN, lincomycin; CFX, ciprofloxacin; NFX, norfloxacin; OFX, ofloxacin. NA indicates non-availability of data because the biotransformation of MPs by the corresponding ammonia oxidizers was not fitted well with the model.

### 3.2. Transformation product identification of LIN and FQs

To identify the TPs of LIN, suspect screening was carried out on the biotransformation samples of single compounds by AOA, AOB, and comammox. The information about TPs, including mass spectra, elemental formula, fragment ion and possible structure, is described in Table 1, whereas peak areas during treatments and possible pathways are presented in Fig. 3 and Fig. 4.

In the LIN biotransformation by comammox, three possible LIN TP candidates were obtained. One plausible LIN TP candidate had an exact mass of [M+H] at 423.2154 (designated as "TP423") and a chemical formula of $C_{18}H_{34}O_7N_2S_1$ (+O from LIN), but had two different retention times (1.75 min and 2.8 min, see Table 1). These two retention times suggest that there are two isomers of TP423 being formed during comammox biotransformation. A molecular ion of m/z 423 with two domain fragment ions (m/z =126.13 and 359.21) was previously identified in the co-composing of LIN mycelia dregs as LIN's hydroxylation at the methylthio group (Calza et al., 2012; Ren et al., 2019). According to the fragment ions, TP423 at 1.75 min in this study might have been generated from LIN hydroxylation at the methylthio group or S-oxidation of LIN (Spizek and Rezanka, 2017) (Table 1), and TP423 at 2.8 min might have been obtained by hydroxylation of the methyl group of the carboxamide moiety (Table 1 and Fig. 4A). Ranitidine was also reported to be transformed into ranitidine S-oxide by AOA (Men et al., 2016). The second possible TP candidate had an exact mass of [M-$H_2O$+H] at 359.2168 (designated as "TP359") and a chemical formula of $C_{17}H_{32}O_7N_2$ (-$CH_2S$+O from LIN) at low abundance. LIN TP359 was generated via demethylthioation and hydroxylation of LIN. The third possible LIN TP candidate had an exact mass of [M+H] at 393.2055 (designated as "TP393") and a chemical formula of $C_{17}H_{32}O_6N_2S_1$ (-$CH_2$ from LIN), which might have been generated by demethylation of LIN by AOM. The demethylation of LIN was also hypothesized in the co-metabolism system using a sequencing batch biofilm reactor (Li et al., 2016). Based on the fragment ion (112.1119), TP393 had two possible structures: N-demethylation or demethylation in the propylchain (Table 1 and Fig. 4A).

For AOA, two possible LIN TP candidates were obtained. One possible TP candidates was TP393. Another previously unidentified possible LIN TP candidate had an exact mass of [M+H] at 423.2443 (designated as "TP423-3") and a chemical formula of $C_{18}H_{34}O_7N_2S_1$ (+O from LIN). However, TP423-3 had a different retention time with the two TP423 isomers identified in the comammox treatment, which suggested that TP423-3 might be another isomer of TP423. Three possible structures of LIN TP423 have been reported in a previous study, including propylchain hydroxylation, hydroxylation of thiomethyl moiety, and hydroxylation of the methyl group of the carboxamide moiety (Calza et al., 2012). The AOB pure culture used in this study cannot biotransform LIN, so no TPs were identified. Generally, we identified LIN TP423 as hydroxylation, LIN TP393 as demethylation, and LIN TP359 as demethylthioation and hydroxylation (Fig. 4A).

To identify the TPs of CFX, NFX, and OFX, suspect screening was carried out on the biotransformation samples of single compounds by AOA, AOB, and comammox (Table 1 and Fig. 3). In the AOA treatment of CFX, two possible TP candidates were detected. One major CFX TP candidate during the AOA treatment had an exact mass of [M+H] at 361.1311 (designated as "TP361") and a chemical formula of $C_{17}H_{17}O_4N_4F_1$ (-H+NO from CFX). TP361 might have been generated through nitrosation of the piperazine moiety. Another TP candidate had a low abundance with an exact mass of [M+H] at 263.0827 (designated as "TP263") and a chemical formula of $C_{13}H_{11}O_3N_2F$ (-$C_4H_7N$ from CFX). TP263 might have originated from the cleavage of the piperazine moiety. In the AOB treatment of CFX, although the removal of CFX was less than 20% overall, TP361 was still detected. In the comammox treatment of CFX, no potential TP candidates were detected.

In the AOA treatment of NFX, three potential TP candidates were detected. One TP candidate during NFX biotransformation by AOA had an exact mass of [M+Na] at 518.1532 (designated as "TP518") and a chemical formula of $C_{22}H_{26}O_9N_3F$ (+$C_6H_8O_6$ from NFX). TP518 might thus be a glucuronide conjugate of NFX. TP518 was also detected in the comammox and AOB treatment of NFX with a relatively high abundance, even if the removal of NFX in the AOB treatment was less than 1%. This phenomenon suggests that TP518 might have a much stronger signal abundance than its parent compound and can be identified as a minor TP. In the AOA treatment of NFX, another possible TP candidate was detected, with an exact mass of [M+H] at 349.1306 (designated as "TP349") and a chemical formula of $C_{16}H_{17}O_4N_4F$ (-H+NO from NFX). In the AOA treatment of NFX, the third possible TP candidate had an exact mass of [M+H] at 251.0826 (designated as "TP251") and a

**Table 1**
Mass, chemical formula, fragment ion, and structure of the identified transformation products (TPs) in the treatments by ammonia oxidizers, hydroxylamine ($NH_2OH$) and nitric oxide (NO)

| Compounds | Exact mass ($m/z$) | Adduct | Formula | Fragmentation ions | Structure | Treatment |
|---|---|---|---|---|---|---|
| Lincomycin (LIN) | 407.2206 | H | $C_{18}H_{34}O_6N_2S$ | 126.1274, 359.2179 | 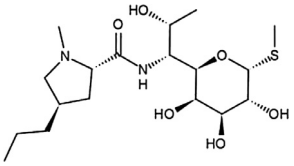 | |
| LIN TP423 | 423.2154 | H | $C_{18}H_{34}O_7N_2S$ | 126.1272 and 359.2180 for retention time (RT) 1.75 min; 126.1275 for RT 2.8 min; 357.2029 for RT 3.13 min. | 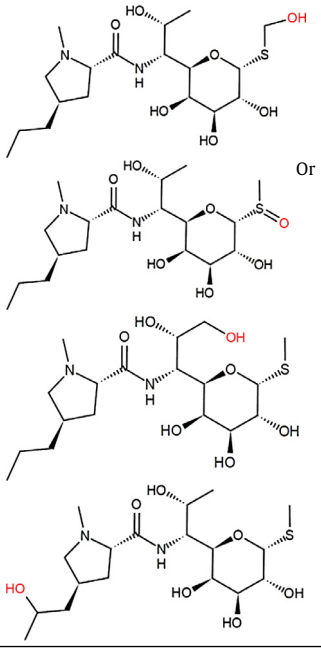 Or | Comammox, AOA, AOA with mixed compounds, $NH_2OH$ |
| LIN TP359 | 359.2168 | M-$H_2O$+H | $C_{17}H_{32}O_7N_2$ | | 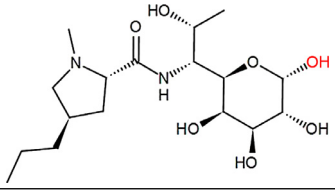 | Comammox |
| LIN TP393 | 393.2055 | H | $C_{17}H_{32}O_6N_2S$ | 112.1119 | 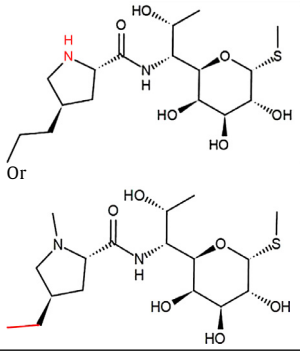 Or | Comammox, AOA, $NH_2OH$, NO |
| Ciprofloxacin (CFX) | 332.1402 | H | $C_{17}H_{18}O_3N_3F$ | 245.1083, 288.1505 | 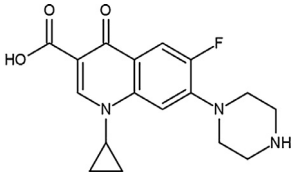 | |

(*continued on next page*)

**Table 1**
(*continued*)

| Compounds | Exact mass (*m/z*) | Adduct | Formula | Fragmentation ions | Structure | Treatment |
|---|---|---|---|---|---|---|
| CFX TP361 | 361.1311 | H | $C_{17}H_{17}O_4N_4F$ | 257.0725, 271.0877 | 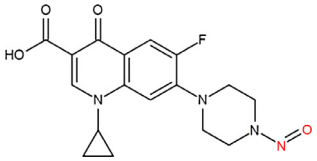 | AOA, AOB, AOA with mixed compounds, $NH_2OH$, NO |
| CFX TP263 | 263.0827 | H | $C_{13}H_{11}O_3N_2F$ | 204.0327; 245.0734 | 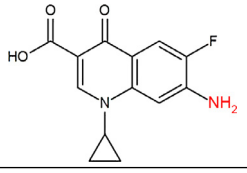 | AOA, $NH_2OH$ |
| CFX TP362 | 362.1347 | H | $C_{17}H_{19}O_6N_3$ | | NA | AOA with mixed compounds |
| CFX TP294 | 294.1248 | H | $C_{14}H_{16}O_3N_3F$ | | 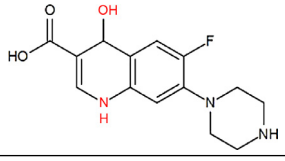 | AOA with mixed compounds, $NH_2OH$ |
| Norfloxacin (NFX) | 320.1405 | H | $C_{16}H_{18}O_3N_3F$ | 205.0769, 233.1082, 302.1300 | 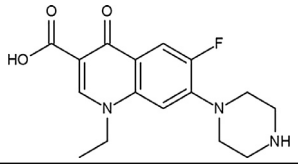 | |
| NFX TP349 | 349.1306 | H | $C_{16}H_{17}O_4N_4F$ | 245.0719; 259.0876 | 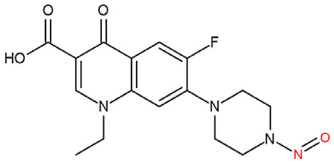 | AOA, AOB, AOA with mixed compounds, $NH_2OH$, NO |
| NFX TP251 | 251.0825 | H | $C_{12}H_{11}O_3N_2F$ | 233.0722 | 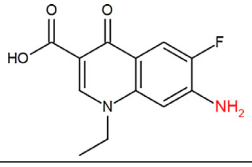 | AOA, $NH_2OH$ |
| NFX TP518 | 518.1532 | Na | $C_{22}H_{26}O_9N_3F$ | | NA | Comammox, AOA, AOB |
| NFX TP350 | 350.1347 | H | $C_{16}H_{19}O_6N_3$ | | NA | AOA with mixed compounds, $NH_2OH$, NO |
| Ofloxacin (OFX) | 362.1506 | H | $C_{18}H_{20}O_4N_3F$ | 261.1032, 318.1611, 344.1403 | 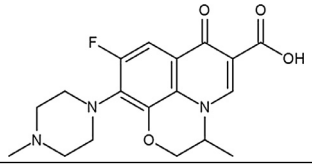 | |
| OFX TP348 | 348.1347 | H | $C_{17}H_{18}O_4N_3F$ | | 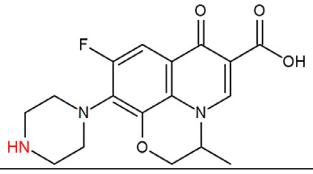 | Comammox, AOA, $NH_2OH$, NO |

NA: not applicable.

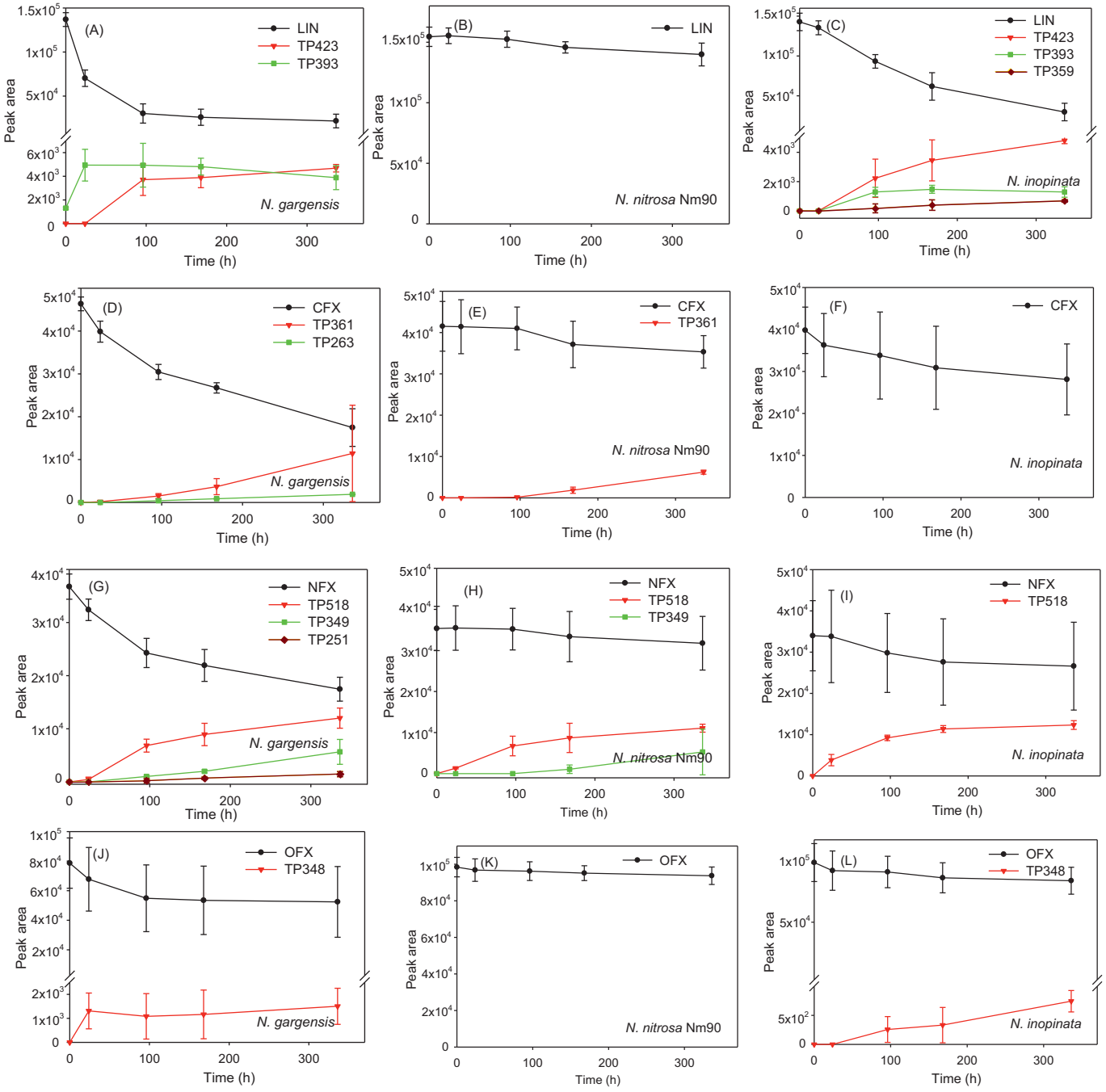


**Fig. 3.** A comparison on biotransformation of LIN (A, B, and C), CFX (D, E, and F), NFX (G, H, and I) and OFX (J, K, and L) by *N. gargensis*, *N. nitrosa* Nm90, and *N. inopinata*, respectively. LIN, lincomycin; CFX, ciprofloxacin; NFX, norfloxacin. TP423, HO-LIN or LIN-S oxide; TP393, demethyl-LIN; TP359, demethylthio-LIN; TP361, nitroso-CFX; TP263 and TP251, likely from the cleavage of piperazine moiety of CFX and NFX, respectively; TP349, nitroso-NFX; TP518, glucuronide-NFX.

chemical formula of $C_{12}H_{11}O_3N_2F$ (-$C_4H_7N$ from NFX). In the comammox treatment of NFX, only TP518 was detected.

In the comammox and AOA treatment of OFX, only one possible TP candidate was detected, with an exact mass of [M+H] at 348.1347 (designated as "TP348") and a chemical formula of $C_{17}H_{18}O_4N_3F$ (-$CH_2$ from OFX). We identified CFX TP361 and NFX TP349 as formed through nitrosation, and OFX TP348 was formed via demethylation (Fig. 4). CFX TP263 and NFX TP251 indicated that the cleavage of the piperazine moiety occurred in the AOA treatment (Fig. 4). CFX TP263 was also identified in the CFX biodegradation of plant tissues, which was generated in two steps: removing $C_2H_2$ at the piperazinyl substituent of CIP via desethylation, followed by the cleavage of the piperazine ring and loss of an $NH_2$ (Yan et al., 2020). Lower removals and different TPs of OFX than those of CFX and NFX in the AOM treatments may have resulted from OFX having a considerably different molecular structure compared to CFX and NFX (Fig. 4).

In general, AOA displayed significant biotransformation for LIN, CFX and NFX; in WWTPs, MPs are usually presented as a cocktail. Therefore, we further conducted the biotransformation of mixed LIN, CFX, and NFX by AOA pure culture to mimic the real environments with mixed MPs. Information about TPs including their mass spectra, elemental formula, fragment ion, and possible structure are presented in Table 1. One possible LIN TP candidate was

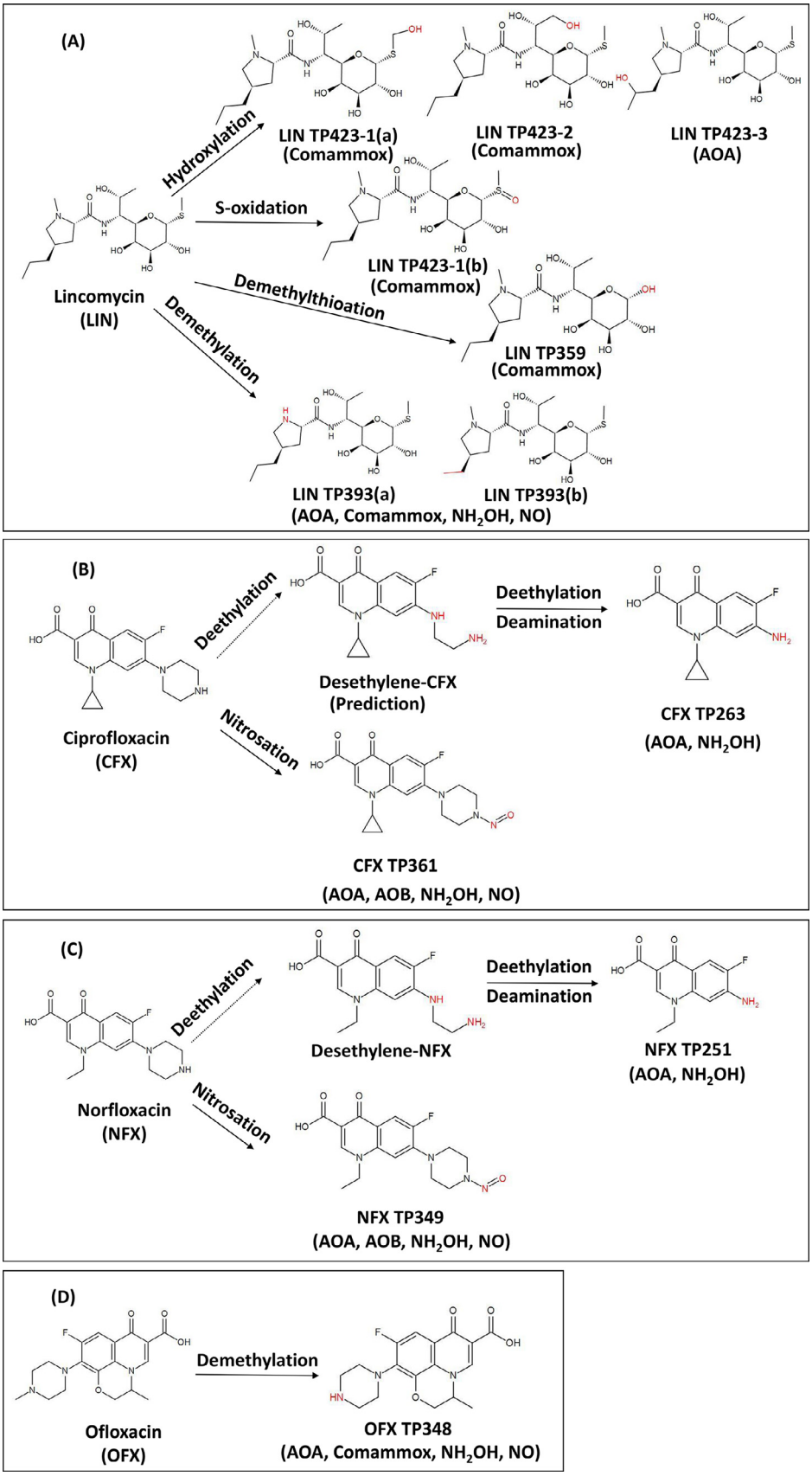


**Fig. 4.** Proposed transformation pathways of LIN (A), CFX (B), NFX (C) and OFX (D) under the treatment of different ammonia oxidizers.

obtained during LIN biotransformation by AOA, with an exact mass of [M+H] at 423.216 (designated as "TP423") and a chemical formula of $C_{18}H_{34}O_7N_2S$ (+O from LIN). Three CFX TP candidates were obtained during CFX biotransformation by the AOA strain. The major CFX TP candidate during CFX biotransformation by AOA had an exact mass of [M+H] at 361.1307 (designated as "TP361") and a chemical formula of $C_{17}H_{17}O_4N_4F_1$ (-H, +NO from CFX). The other two potential candidates had a low abundance, and an exact mass of [M+H] at 362.1347 (designated "TP362"), and a chemical formula of $C_{17}H_{19}O_6N_3$ (-F, +OH, +O, +O from CFX), or an exact mass of [M+H] at 294.1248 (designated as "TP294") and a chemical formula of $C_{14}H_{16}O_3N_3F$ (-$C_3H_2$ from CFX). In heat-inactivated controls, almost no TPs for LIN, CFX, NFX and OFX were found. In abiotic controls, LIN TP423, CFX TP361, CFX TP263, CFX TP294, NFX TP349, NFX TP251, and OFX TP348 were detected at low abundance.

We identified that TP361 was formed through a nitrosation reaction; TP362 was formed through a defluorination reaction, hydroxylations on both the aromatic ring and the piperazinyl group; and TP294 was formed through a dealkylation reaction (naphthenic base). Two NFX TP candidates (TP349 and TP350) biotransformed by AOA were detected, with the exact masses of [M+H] at 349.1307 and 350.1347, and formulae of $C_{16}H_{17}O_4N_4F$ (-H, +NO from NFX) and $C_{16}H_{19}O_6N_3$ (-F, +OH, +O, +O from NFX). TP349 was a nitrosation reaction product of NFX, and TP350 was generated from a defluorination and hydroxylation reactions on both aromatic ring and the piperazinyl group. However, no CFX TP294 (N-dealkylation), CFX TP362, and NFX TP350 were detected in the biotransformation samples of single CFX or NFX by AOA and comammox. There are two possible reasons for those differences of TPs in single and mixed compound experiments. First, low abundance of TP candidates in single compound experiment were obtained due to low injection volume (5 $\mu$m). Second, the biotransformation pattern in mixed MPs condition is different from individual MP addition. These results may provide insights in the MPs biotransformation pattern in real environments.

### 3.3. Transformation pathways of LIN and FQs by three AOM

In general, the biotransformation of LIN and FQs by three AOM in this study were generated via three typical processes (Fig. 4): (i) hydroxylation, S-oxidation, and nitrosation, (ii) demethylation or demethylthioation, and (iii) cleavage of the piperazine moiety. Hydroxylation might have been performed by the AMOs of the ammonia oxidizers. AMOs that convert ammonia to hydroxylamine by adding O are not compound specific (Daims et al., 2015; Hooper et al., 1997; Kozlowski et al., 2016), and they may oxide the MPs by adding O into amide, aromatic ring, or alkyl groups.

The autotrophic nitrification process by-product NO reacts with $O_2^-$ to form $ONOO^-$, which is a strong nitrosating agent responsible for N-nitrosation reactions (Brienza et al., 2020; Heinrich et al., 2013). Nitrite reductases are encoded in the genomes of the three ammonia oxidizers in this study, suggesting that NO might also be generated from $NO_2^-$ by AOA, AOB and comammox. However, comammox can oxidize $NO_2^-$ to $NO_3^-$ (Daims et al., 2015), maintaining a low $NO_2^-$ concentration in the comammox culture and then less NO generated from $NO_2^-$. This is probably why N-nitroso-CFX and N-nitroso-NFX were only detected in AOA and AOB cultures, but not in comammox. Demethylation or demethylthioation might be catalyzed by methyltransferases or methylthiotransferases. Methyltransferases are present in the genomes of *N. gargensis* (AOA) and *N. inopinata* (comammox), whereas methylthiotransferases are only found in the genomes of *N. gargensis* (AOA). Cleavage of the piperazine moiety may have been formed by three steps: deethylation, deamination, and further deethylation. Deamination might be performed by deaminases encoded in the genomes of the three ammonia oxidizers used in the present study. The enzymatic pathway of deethylation, such as through specific enzymes or methyltransferases should be investigated in future research.

### 3.4. Abiotic transformation of target MPs by $NH_2OH$ and NO

Hydroxylamine is an important intermediate in ammonia oxidation by AOA, AOB, and comammox (Kozlowski et al., 2016; Vajrala et al., 2013). To test whether MPs abiotically react with hydroxylamine, abiotic transformation experiments were performed by adding $NH_2OH$ (10 $\mu$M $NH_2OH$ at 12 h) (Fig. 5). LIN, CFX, NFX, and OFX were removed by $NH_2OH$, with removals above 90% (Fig. 5 and Fig. S4).

Hydroxylamine is often used as a promoter in Fenton-like technology, and the hydroxyl radical is the principal component that attacks target pollutants (such as LIN and chloramphenicol) in these systems (Hou et al., 2017; Ouyang et al., 2020). Hydroxylamine might enhance the generation of hydroxyl radicals which results in the degradation of target MPs by hydroxylamine. In contrast to abiotic transformation by $NH_2OH$, AOA *N. gargensis* cannot biotransform OFX, AOB cannot biotransform LIN and OFX, and comammox *N. inopinata* cannot biotransform CFX, NFX, and OFX (removal rate <20%). These results suggest that the concentrations of extracellular hydroxylamine available for MPs in the AOM treatment were relatively low compared to the experimental concentrations (10 $\mu$M $NH_2OH$). In a previous study, extracellular $NH_2OH$ concentrations in the medium of *N. gargensis* (2 mM $NH_4^+$, incubation for 58 h), *N. nitrosa* Nm90 (2 mM $NH_4^+$, incubation for 58 h), and *N. inopinata* (2 mM $NH_4^+$, incubation for 48 h) were approximately 0.33 $\mu$M, not detected and 0.43 $\mu$M, respectively (Liu et al., 2017). Even though no $NH_2OH$ was detected in *N. nitrosa* Nm90, other AOB such as *N. multiformis* were identified to produce relatively high extracellular $NH_2OH$ concentrations (2.2 $\mu$M) in the medium (Liu et al., 2017). Although the concentrations of extracellular $NH_2OH$ in the comammox treatment in this study might have been higher than those in the AOA treatment, CFX and NFX removals in the AOA treatment were higher than those in the comammox (Fig. 3). This suggests that the CFX and NFX removal in the AOA treatment was mainly conducted by AOA rather than abiotically by $NH_2OH$ in the medium.

Further analyses of the TPs of LIN and FQs in the $NH_2OH$-treated fresh medium were performed. TP423 and TP393 for LIN, TP361, TP263 and TP294 for CFX, TP349, TP251, and TP350 for NFX, and TP348 for OFX detected during biotransformation treatments were also identified in the fresh medium amended with $NH_2OH$ (Fig. 5). A high abundance of CFX TP263 was detected in the $NH_2OH$ treatment (Fig. 5), but CFX TP263 was only found in the AOA treatment at a low abundance instead of the comammox and AOB treatment (Fig. 3). This result indicates that CFX transformation in AOA treatment might have been mainly generated through enzymatic conversions instead of abiotic conversion through $NH_2OH$. CFX TP361 was detected in the $NH_2OH$ treatment (Fig. 5), but CFX TP361 was only found in the AOA and AOB treatments instead of the comammox (Fig. 3). Combining the extracellular $NH_2OH$ concentrations in AOA, AOB, and comammox in this study, the CFX transformation in the AOB treatment might have mainly been generated through enzymatic conversions instead of $NH_2OH$. The LIN removals in the AOA and comammox treatments were similar, with no removal of LIN in the AOB (Fig. 3). Other LIN TPs including LIN TP423 and LIN TP393 might have been generated by both enzymatic conversions and $NH_2OH$. In general, high concentrations of the intermediate $NH_2OH$ can transform LIN and FQs. In addition to enzymatic reactions, abiotic degradation also contributed to the transformation of LIN and FQs during ammonia oxidation. However, extracellular $NH_2OH$ in natural environments

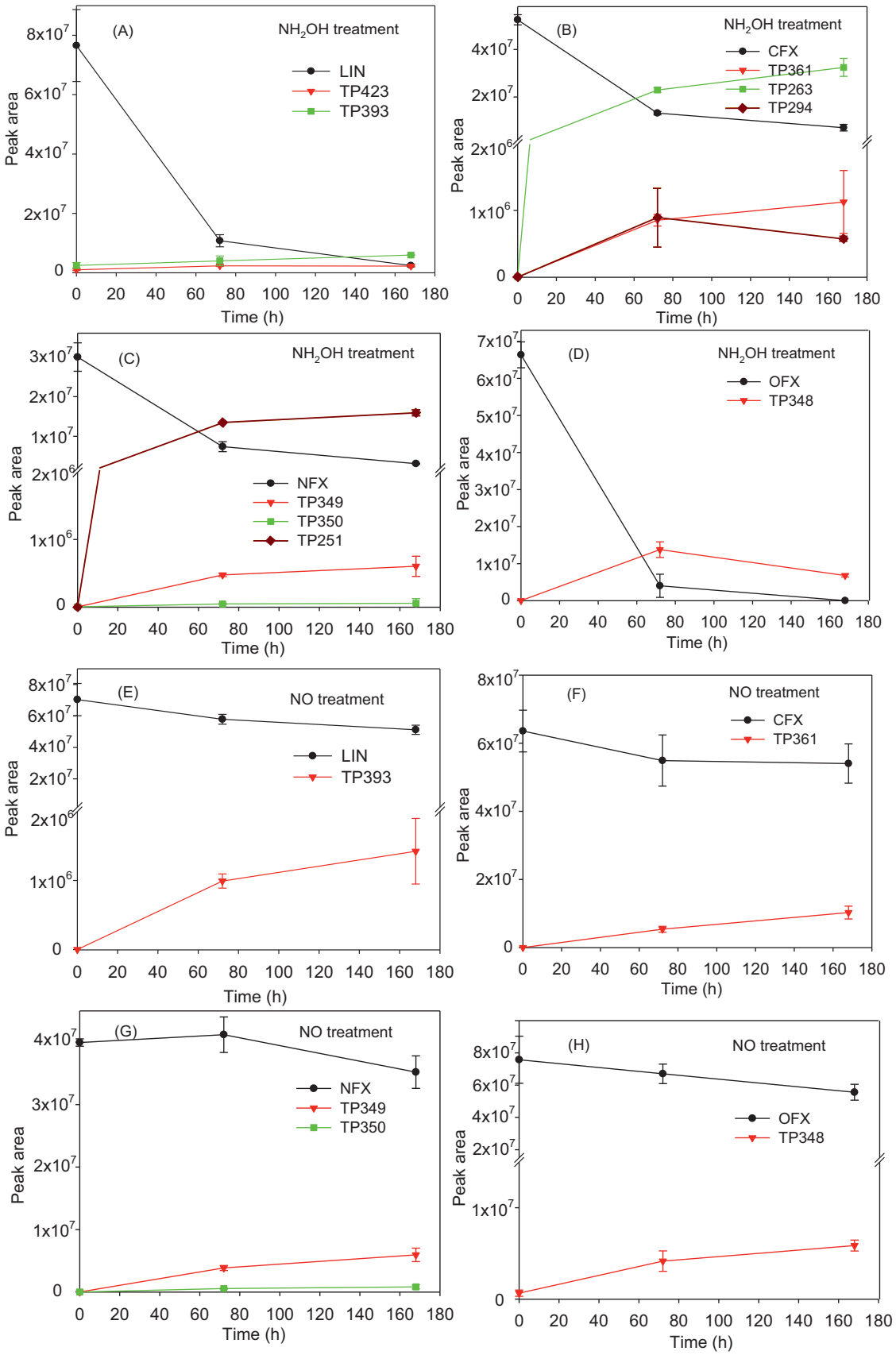


**Fig. 5.** Removal of target MPs by addition of $NH_2OH$ (10 $\mu$M every12 h) and NO (200 $\mu$M in 168 h) abiotically. LIN, lincomycin; CFX, ciprofloxacin; NFX, norfloxacin; OFX, ofloxacin. TP423, HO-LIN or LIN-S-oxide; TP393, demethyl-LIN; TP361, nitroso-CFX; TP263, likely from the cleavage of piperazine moiety; TP349, nitroso-NFX; TP350, defluoro and hydroxyl-NFX; TP251, likely from the cleavage of piperazine moiety; TP348, demethyl-OFX. The structure of CFX TP294 remains unclear.

rarely reaches the high concentrations needed and might thus contribute only a small part to the transformation potential of LIN and FQs.

NO is another important intermediate in ammonia oxidation by AOA, AOB, and comammox (Kits et al., 2019; Kozlowski et al., 2016). To test whether MPs abiotically react with NO, abiotic transformation experiments were performed by adding an amount of NO (200 $\mu$M $NH_2OH$ at 168 h) (Fig. 5). The removals of LIN, CFX, NFX, and OFX by NO were relatively low, ranging from 12% ± 8% to 26% ± 11% (Fig. 5 and Fig. S4). Further analyses of the TPs of LIN and FQs in the NO-treated fresh medium were performed. TP393 for LIN, TP361 for CFX, TP349 and TP 350 for NFX, and TP 348 for OFX detected in the biotransformation treatments by ammonia oxidizers were also identified in the basal medium added with NO (Fig. 5). Moreover, CFX TP361 and NFX TP349 detected in NO-treatments than in $NH_2OH$ treatments further indicated that N-nitroso-CFX and N-nitroso-NFX can be generated through reaction with NO. LIN TP393 and OFX TP348 indicated that demethylation occurred in the NO treatment.

### 3.5. Environmental relevance and implications

Considering the adverse effects of FQs in the sludge and sediment, enhancing the degradation and detoxification of FQs in WWTPs and aquatic environments is desirable. Biodegradation is one of the most economically and environmentally friendly ways to eliminate these contaminants. However, few efficient degrading strains for LIN and FQs have been isolated so far (Wang et al., 2018).

Many studies have shown that the biodegradation of MPs by ammonia oxidizers follows the co-metabolic mechanism (Han et al., 2019; Xu et al., 2016; Yu et al., 2018; Zhou et al., 2019a). For activated amide- containing MPs, there are a variety of biotransformation reactions, including amide hydrolysis, ester hydrolysis, dehalogenation, N-dealkylation, hydroxylation, oxidation, nitro reduction and glutathione conjugation (Helbling et al., 2010).

The AOA strain possessed the best biotransformation capability of MPs. In this study, LIN was effectively removed by the AOA and comammox strains, but not by AOB; FQs were most significantly removed by the AOA, followed by comammox and AOB. AOA has a higher substrate affinity than many AOB strains and a higher cell growth rate compared to comammox and might thus play a more important role in the biotransformation of MPs by ammonia oxidizers in the environment. Moreover, the ammonia/MP ratio might have affected the removal rate. After cometabolic transformation of MPs by ammonia oxidizers, some TPs might have degraded into small molecules by other microbes. In the environment including WWTPs, surface water and soil, the concentrations of MPs were much lower than those of ammonia.

Notably, many TPs might still display antimicrobial activities. In this study, most TP candidates were generated via hydroxylation, nitrosation, ring cleavage, and demethylation. However, if the antimicrobially active structures of the parent compound are not destroyed in the TPs, they are still proposed to possess antibiotic activities. For example, the carboxyl and ketone groups of FQs, i.e., antimicrobially active moieties, are well preserved in CFX TP263, CFX TP361, CFX TP349, and NFX TP251 (likely from the cleavage of the piperazine ring), although the loss of the piperazine ring influences the biological spectrum (Domagala, 1994). Additionally, some TPs, such as glucuronide-FQs and nitroso-FQs, might be transformed back to their parent compounds. Consequently, potential TPs formed through MP biotransformation by ammonia oxidizers and their activity and toxicity should be evaluated in the future.

## 4. Conclusion

In this study, we demonstrate the biotransformation abilities and biochemical pathways of lincomycin (LIN) and three fluoroquinolone antibiotics (FQs)by three different ammonia oxidizers. The AOA strain *N. gargensis* presented the best biotransformation abilities of LIN and FQs, followed by comammox and AOB strains. The transformation products were likely formed via (i) hydroxylation, S-oxidation, or nitrosation, (ii) demethylation or demethylthioation, and (iii) cleavage of the piperazine moiety. The ammonia-oxidizing intermediate hydroxylamine can abiotically react with LIN and FQs, whereas the intermediate NO was involved in the formation of N-notroso products of ciprofloxacin and norfloxacin. However, these abiotic transformation reactions contribute less to LIN and FQ removal by AOM compared with the enzymatic conversions. Ecological toxicity and risk of LIN and FQs' TPs during the biotransformation should be further evaluated.

## Declaration of Competing Interest

The authors declare no conflict of interest.

## Acknowledgements

We would like to thank National Natural Science Foundation of China (Grant No. 31770551, 41807465, 41725002, 41730646, 42030411, 31400451 and 41761144062). Dr. Uli Klümper was supported by the ANTIVERSA project funded by the German Federal Ministry of Education and Research (BMBF) under grant number 01LC1904A. Responsibility for the information and views expressed in the manuscript lies entirely with the authors. The Project of Young Scientist Group of NIGLAS (2021NIGLAS-CJH01) also financially sponsored the research. We would like to thank Prof. Michael Wagner from the University of Vienna for providing resources for carrying out the mixed-compounds biotransformation experiments. Dr. Lei Chen and Dr. Xin Li at the Instrumental Analysis Center, Shanghai Jiao Tong University are acknowledged for their assistance with LC- QToF MS analyses.

## Supplementary materials

Supplementary material associated with this article can be found, in the online version, at doi:10.1016/j.watres.2021.117003.

## References

Bengtsson-Palme, J., Larsson, D.G.J, 2016. Concentrations of antibiotics predicted to select for resistant bacteria: Proposed limits for environmental regulation. Environ. Int. 86, 140–149.

Brienza, M., Manasfi, R., Sauvêtre, A., Chiron, S., 2020. Nitric oxide reactivity accounts for N-nitroso-ciprofloxacin formation under nitrate-reducing conditions. Water Res 185, 116293.

Calza, P., Medana, C., Padovano, E., Dal Bello, F., Baiocchi, C, 2012. Identification of the unknown transformation products derived from lincomycin using LC-HRMS technique. J. Mass Spectrom. 47 (6), 751–759.

Caranto, J., Lancaster, K., 2017. Nitric oxide is an obligate bacterial nitrification intermediate produced by hydroxylamine oxidoreductase. P. Natl. Acad. Sci. USA 114 (31), 8217–8222.

Chao, Y.Q., Mao, Y.P., Yu, K., Zhang, T., 2016. Novel nitrifiers and comammox in a full-scale hybrid biofilm and activated sludge reactor revealed by metagenomic approach. Appl. Microbiol. Biot. 100 (18), 8239.

Chen, J., Liu, Y.S., Zhang, J.N., Yang, Y.Q., Hu, L.X., Yang, Y.Y., Zhao, J.L., Chen, F.R., Ying, G.G., 2017. Removal of antibiotics from piggery wastewater by biological aerated filter system: Treatment efficiency and biodegradation kinetics. Bioresour. Technol. 238, 70–77.

D'Alessio, M., Durso, L.M., Miller, D.N., Woodbury, B., Ray, C., Snow, D.D., 2019. Environmental fate and microbial effects of monensin, lincomycin, and sulfamethazine residues in soil. Environ. Pollut. 246, 60–68.

Daims, H., Lebedeva, E.V., Pjevac, P., Han, P., Herbold, C., Albertsen, M., Jehmlich, N., Palatinszky, M., Vierheilig, J., Bulaev, A., Kirkegaard, R.H., von Bergen, M., Rattei, T., Bendinger, B., Nielsen, P.H., Wagner, M., 2015. Complete nitrification by *Nitrospira bacteria*. Nature 528 (7583), 504–509.

Danner, M.C., Robertson, A., Behrends, V., Reiss, J., 2019. Antibiotic pollution in surface fresh waters: Occurrence and effects. Sci. Total Environ. 664, 793–804.
Domagala, J.M., 1994. Structure-activity and structure-side-effect relationships for the quinolone antibacterials. J. Antimicrob. Chemother. 33 (4), 685–706.
Gao, L.H., Shi, Y.L., Li, W.H., Liu, J.M., Cai, Y.Q., 2012. Occurrence, distribution and bioaccumulation of antibiotics in the Haihe River in China. J. Environ. Monit. 14 (4), 1248–1255.
Gonzalez-Pleiter, M., Gonzalo, S., Rodea-Palomares, I., Leganes, F., Rosal, R., Boltes, K., Marco, E., Fernandez-Pinas, F., 2013. Toxicity of five antibiotics and their mixtures towards photosynthetic aquatic organisms: Implications for environmental risk assessment. Water Res 47 (6), 2050–2064.
Grenni, P., Ancona, V., Caracciolo, A.B., 2018. Ecological effects of antibiotics on natural ecosystems: A review. Microchem. J. 136, 25–39.
Han, P., Yu, Y., Zhou, L., Tian, Z., Li, Z., Hou, L., Liu, M., Wu, Q., Wagner, M., Men, Y., 2019. Specific micropollutant biotransformation pattern by the comammox bacterium *Nitrospira inopinata*. Environ. Sci. Technol. 53 (15), 8695–8705.
Hatzenpichler, R., Lebedeva, E.V., Spieck, E., Stoecker, K., Richter, A., Daims, H., Wagner, M., 2008. A moderately thermophilic ammonia-oxidizing crenarchaeote from a hot spring. P. Natl. Acad. Sci. USA 105 (6), 2134–2139.
He, J.Z., Hu, H.W., Zhang, L.M., 2012. Current insights into the autotrophic thaumarchaeal ammonia oxidation in acidic soils. Soil Biol. Biochem. 55, 146–154.
Heinrich, T.A., da Silva, R.S., Miranda, K.M., Switzer, C.H., Wink, D.A., Fukuto, J.M., 2013. Biological nitric oxide signalling: chemistry and terminology. Brit. J. Pharmacol. 169 (7), 1417–1429.
Helbling, D.E., Hollender, J., Kohler, H.-P.E., Fenner, K., 2010. Structure-based interpretation of biotransformation pathways of amide-containing compounds in sludge-seeded bioreactors. Environ. Sci. Technol. 44 (17), 6628–6635.
Helbling, D.E., Johnson, D.R., Honti, M., Fenner, K., 2012. Micropollutant Biotransformation Kinetics Associate with WWTP Process Parameters and Microbial Community Characteristics. Environ. Sci. Technol. 46 (19), 10579–10588.
Hooper, A.B., Vannelli, T., Bergmann, D.J., Arciero, D.M., 1997. Enzymology of the oxidation of ammonia to nitrite by bacteria. Anton. Leeuw. 71, 59–67.
Hou, X.J., Huang, X.P., Jia, F.L., Ai, Z.H., Zhao, J.C., Zhang, L.Z., 2017. Hydroxylamine promoted goethite surface fenton degradation of organic pollutants. Environ. Sci. Technol. 51 (9), 5118–5126.
Kandeler, E., Gerber, H., 1988. Short-term assay of soil urease acticity using colorimetric determination of ammonium. Biol. Fert. Soils 6 (1), 68–72.
Kits, K.D., Jung, M.-Y., Vierheilig, J., Pjevac, P., Sedlacek, C.J., Liu, S., Herbold, C., Stein, L.Y., Richter, A., Wissel, H., Brüggemann, N., Wagner, M., Daims, H., 2019. Low yield and abiotic origin of $N_2O$ formed by the complete nitrifier *Nitrospira inopinata*. Nat. Commun. 10, 1836.
Kits, K.D., Sedlacek, C.J., Lebedeva, E.V., Han, P., Bulaev, A., Pjevac, P., Daebeler, A., Romano, S., Albertsen, M., Stein, L.Y., Daims, H., Wagner, M., 2017. Kinetic analysis of a complete nitrifier reveals an oligotrophic lifestyle. Nature 549 (7671), 269–272.
Klumper, U., Recker, M., Zhang, L.H., Yin, X.L., Zhang, T., Buckling, A., Gaze, W.H., 2019. Selection for antimicrobial resistance is reduced when embedded in a natural microbial community. ISME J 13 (12), 2927–2937.
Koops, H.P., Bottcher, B., Moller, U.C., Pommereningroser, A., Stehr, G., 1991. Classification of 8 new species of ammonia-oxidizing bacteria: *Nitrosomonas communis* sp. nov., *Nitrosomonas ureae* sp. nov., *Nitrosomonas aestuarii* sp. nov., *Nitrosomonas marina* sp. nov., *Nitrosomonas nitrosa* sp. nov., *Nitrosomonas eutropha* sp. nov., *Nitrosomonas oligotropha* sp. nov. and *Nitrosomonas halophila* sp. nov. J. Gen. Microbiol. 137, 1689–1699.
Kozlowski, J.A., Stieglmeier, M., Schleper, C., Klotz, M.G., Stein, L.Y., 2016. Pathways and key intermediates required for obligate aerobic ammonia-dependent chemolithotrophy in bacteria and Thaumarchaeota. ISME J 10 (8), 1836–1845.
Kümmerer, K., 2009. Antibiotics in the aquatic environment – A review – Part I. Chemosphere 75 (4), 417–434.
Li, Y., Zhou, J., Gong, B., Wang, Y., He, Q., 2016. Cometabolic degradation of lincomycin in a sequencing batch biofilm reactor (SBBR) and its microbial community. Bioresour. Technol. 214, 589–595.
Liu, J.Y., Li, X.Q., Wang, X., 2019. Toxicological effects of ciprofloxacin exposure to *Drosophila melanogaster*. Chemosphere 237, 124542.
Liu, S.F., Wang, H.Y., Chen, L.M., Wang, J.W., Zheng, M.S., Liu, S.T., Chen, Q., Ni, J.R., 2020. Comammox *Nitrospira* within the Yangtze River continuum: community, biogeography, and ecological drivers. ISME J 14 (10), 2488–2504.
Liu, S.R., Han, P., Hink, L., Prosser, J.I., Wagner, M., Bruggemann, N., 2017. Abiotic conversion of extracellular $NH_2OH$ contributes to $N_2O$ emission during ammonia oxidation. Environ. Sci. Technol. 51 (22), 13122–13132.
Liu, X., Lu, S., Guo, W., Xi, B., Wang, W., 2018. Antibiotics in the aquatic environments: A review of lakes. China. Sci. Total Environ. 627, 1195–1208.
Martens-Habbena, W., Berube, P.M., Urakawa, H., de, J.R., Stahl, D.A., 2009. Ammonia oxidation kinetics determine niche separation of nitrifying archaea and bacteria. Nature 461 (7266), 976–979.
Men, Y.J., Han, P., Helbling, D.E., Jehmlich, N., Herbold, C., Gulde, R., Onnis-Hayden, A., Gu, A.Z., Johnson, D.R., Wagner, M., Fenner, K., 2016. Biotransformation of two pharmaceuticals by the ammonia-oxidizing archaeon *Nitrososphaera gargensis*. Environ. Sci. Technol. 50 (9), 4682–4692.
Miranda, K.M., Espey, M.G., Wink, D.A., 2001. A rapid, simple spectrophotometric method for simultaneous detection of nitrate and nitrite. Nitric Oxide-Biol. Chem. 5 (1), 62–71.
Mirzaei, R., Mesdaghinia, A., Hoseini, S.S., Yunesian, M., 2019. Antibiotics in urban wastewater and rivers of Tehran, Iran: Consumption, mass load, occurrence, and ecological risk. Chemosphere 221, 55–66.
Mussmann, M., Brito, I., Pitcher, A., Sinninghe-Damste, J., Hatzenpichler, R., Richter, A., Nielsen, J., Nielsen, P., Müller, A., Daims, H., Wagner, M., Head, I., 2011. Thaumarchaeotes abundant in refinery nitrifying sludges express amoA but are not obligate autotrophic ammonia oxidizers. P. Natl. Acad. Sci. USA 108, 16771–16776.
Naslund, J., Hedman, J.E., Agestrand, C., 2008. Effects of the antibiotic ciprofloxacin on the bacterial community structure and degradation of pyrene in marine sediment. Aquat. Toxicol. 90 (3), 223–227.
Ouyang, Q., Lian, J.T., Lu, B.Z., Fang, Z.Q., 2020. Effects and mechanisms of lincomycin degradation by six promoters in the mZVI/$H_2O_2$ systems. Chem. Eng. J. 387, 123417.
Pjevac, P., Schauberger, C., Poghosyan, L., Herbold, C., van Kessel, A.H.J., Daebeler, M., Steinberger, A., Jetten, M., Lücker, M., Wagner, M., S., Daims, H, 2017. AmoA-targeted polymerase chain reaction primers for the specific detection and quantification of comammox *Nitrospira* in the environment. Front. Microbiol. 8, 1508–1518.
Prosser, J.I., Nicol, G.W., 2012. Archaeal and bacterial ammonia-oxidisers in soil: the quest for niche specialisation and differentiation. Trends Microbiol 20 (11), 523–531.
Ren, S., Lu, A., Guo, X., Zhang, Q., Wang, Y., Guo, X., Wang, L., Zhang, B., 2019. Effects of co-composting of lincomycin mycelia dregs with furfural slag on lincomycin degradation, degradation products, antibiotic resistance genes and bacterial community. Bioresour. Technol. 272, 83–91.
Rodriguez-Mozaz, S., Chamorro, S., Marti, E., Huerta, B., Gros, M., Sanchez-Melsio, A., Borrego, C.M., Barcelo, D., Luis Balcazar, J., 2015. Occurrence of antibiotics and antibiotic resistance genes in hospital and urban wastewaters and their impact on the receiving river. Water Res 69, 234–242.
Rusch, M., Spielmeyer, A., Zorn, H., Hamscher, G., 2018. Biotransformation of ciprofloxacin by *Xylaria longipes*: structure elucidation and residual antibacterial activity of metabolites. Appl. Microbiol. Biot. 102, 8573–8584.
Rusch, M., Spielmeyer, A., Zorn, H., Hamscher, G., 2019. Degradation and transformation of fluoroquinolones by microorganisms with special emphasis on ciprofloxacin. Appl. Microbiol. Biot. 103 (17), 6933–6948.
Sarmah, A.K., Meyer, M.T., Boxall, A.B.A, 2006. A global perspective on the use, sales, exposure pathways, occurrence, fate and effects of veterinary antibiotics (VAs) in the environment. Chemosphere 65 (5), 725–759.
Spizek, J., Rezanka, T., 2017. Lincosamides: Chemical structure, biosynthesis, mechanism of action, resistance, and applications. Biochem. Pharmacol. 133, 20–28.
Vajrala, N., Martens-Habbena, W., Sayavedra-Soto, L.A., Schauer, A., Bottomley, P.J., Stahl, D.A., Arp, D.J., 2013. Hydroxylamine as an intermediate in ammonia oxidation by globally abundant marine archaea. P. Natl. Acad. Sci. USA 110 (3), 1006–1011.
Wang, M., Cai, C., Bo, Z., Liu, H., 2018. Characterization and mechanism analysis of lincomycin biodegradation with *Clostridium* sp. strain LCM-B isolated from lincomycin mycelial residue (LMR). Chemosphere 193, 611–617.
Wang, M., Liu, H., Dai, X., 2020. Dosage effects of lincomycin mycelial residues on lincomycin resistance genes and soil microbial communities. Environ. Pollut. 256, 113392.
Xu, Y.F., Yuan, Z.G., Ni, B.J., 2016. Biotransformation of pharmaceuticals by ammonia oxidizing bacteria in wastewater treatment processes. Sci. Total Environ. 566, 796–805.
Yan, Y., Pengmao, Y., Xu, X., Zhang, L., Wang, G., Jin, Q., Chen, L., 2020. Migration of antibiotic ciprofloxacin during phytoremediation of contaminated water and identification of transformation products. Aquat. Toxicol. 219, 105374.
Yang, X.L., Li, Y.B., Wang, X., 2020. Effects of ciprofloxacin exposure on the earthworm *Eisenia fetida*. Environ. Pollut. 262, 114287.
Yu, Y., Han, P., Zhou, L.-J., Li, Z., Wagner, M., Men, Y., 2018. Ammonia monooxygenase-mediated cometabolic biotransformation and hydroxylamine-mediated abiotic transformation of micropollutants in an AOB/NOB Coculture. Environ. Sci. Technol. 52 (16), 9196–9205.
Zhang, S.B., Qin, W., Xia, X.H., Xia, L.Z., Li, S.L., Zhang, L.W., Bai, Y.B., Wang, G.Q., 2020. Ammonia oxidizers in river sediments of the Qinghai-Tibet Plateau and their adaptations to high-elevation conditions. Water Res 173, 115589.
Zhao, M.M., Chen, Y.P., Xue, L.G., Fan, T.T., 2020. Three kinds of ammonia oxidizing microorganisms play an important role in ammonia nitrogen self-purification in the Yellow River. Chemosphere 243, 125405.
Zhi, S., Zhou, J., Yang, F., Tian, L., Zhang, K., 2018. Systematic analysis of occurrence and variation tendency about 58 typical veterinary antibiotics during animal wastewater disposal processes in Tianjin. China. Ecotox. Environ. Safe 165, 376–385.
Zhou, L.-J., Han, P., Yu, Y., Wang, B., Men, Y., Wagner, M., Wu, Q.L., 2019a. Cometabolic biotransformation and microbial-mediated abiotic transformation of sulfonamides by three ammonia oxidizers. Water Res 159, 444–453.
Zhou, L.-J., Wu, Q.L., Zhang, B.-B., Zhao, Y.-G., Zhao, B.-Y., 2016. Occurrence, spatiotemporal distribution, mass balance and ecological risks of antibiotics in subtropical shallow Lake Taihu. China. Environ. Sci. Proc. Imp. 18 (4), 500–513.
Zhou, L.-J., Ying, G.-G., Liu, S., Zhao, J.-L., Yang, B., Chen, Z.-F., Lai, H.-J., 2013. Occurrence and fate of eleven classes of antibiotics in two typical wastewater treatment plants in South China. Sci. Total Environ. 452, 365–376.
Zhou, L.-J., Ying, G.-G., Zhao, J.-L., Yang, J.-F., Wang, L., Yang, B., Liu, S., 2011. Trends in the occurrence of human and veterinary antibiotics in the sediments of the Yellow River, Hai River and Liao River in northern China. Environ. Pollut. 159 (7), 1877–1885.
Zhou, L.J., Li, J., Zhang, Y.D., Kong, L.Y., Jin, M., Yang, X.D., Wu, Q.L.L, 2019b. Trends in the occurrence and risk assessment of antibiotics in shallow lakes in the lower-middle reaches of the Yangtze River basin, China. Ecotox. Environ. Safe 183, 109511.